Fast technique of linear microwave circuit phase extraction from magnitude

F Liu, B. Ravelo

Fast technique of linear microwave circuit phase extraction from magnitude

F. Liu and B. Ravelo

Nanjing University of Information Science & Technology (NUIST),

Nanjing, Jiangsu 210044, China

e-mail: blaise.ravelo@nuist.edu.cn

Abstract

A phase shift (PS) extraction technique from magnitude spectrum is developed in the present paper. The proposed technique is based on the geometrical analysis of equivalent vectors represented by the unknown and reference signal magnitudes measured with spectrum analyzer in the given operation frequency band. By considering the cosine theorem, a formula allowing to extract PS of the tested arbitrary signals is established. Extracted PS accuracy analyses with respect to the power combiner reflection and isolation are performed. The feasibility test was carried out in the frequency band defined from 3 Hz to 0.6 GHz. As expected, the obtained result validates the proposed PS extraction with a good fitting between the calculated transmission phase and simulations. In the future, this technique can be good candidate useful for the EMC and signal integrity analyses of embedded printed circuit boards.

Keywords: Phase shift (PS), extraction technique of phase shift (ETPS), RF/microwave circuit, methodology, measurement technique.

Acknowledgements

This research work was supported by NSFC (61601233 and 61750110535), by NSF of Jiangsu (BK20150918), by Jiangsu Innovation and Enterprise Group Talents Plan 2015 (SRCB201526), by Defense Research Foundation (6140209050116ZK53001) and by PAPD.

1. Introduction

Since 1960s, the phase shift (PS) measurement is one of the key points of the RF and microwave communication system performance [1-2]. After the static phase measurement, dynamic PS technique by using synchronized PIN diodes [1] was become a revolutionary method for the microwave engineers. Then, further technique based on the stepped phase modulation was also proposed [2]. Over the decades, the progress of the RF/microwave system is also linked by the design process of the phase shifters with various techniques in millimeter wave [3-5], development of vector sum PS approach [6], design zero delay PS [7], implementation of robust time/phase synchronization process [8] and improvement of electromagnetic radiated wave technique [9-10]. Nowadays, behind the energy consumption optimization, the efficiency tradeoff of wireless communication depends indirectly to the phase shifters [11]. The phase shifter function constitutes also a solution key for diverse electrical systems as the design of low loss power electronic converter [12].

Despite the quasi-omnipresence of the phase shifters in all electronic systems, the PS measurement knows a lot of diversity of techniques especially in link with the range of the application frequency bands from some Hertz to optical frequency bands [13-31]. The most expanded PS measurement techniques can be found in the Tera-Hertz optical engineering are developed with the interferometry technique [13-21]. The technique was applied to various applications as visualization of biological molecules with thin lubricant films [13], optical wavefront reconstruction [14], optical phase-grating multiplexing [15], spiral patterns with single shot phase shifting [16], frequency scanning laser [17], development of algorithm with unknown reference phases [18], decoding method [19], surface micro-topography measurement [20] and THz-wave phase shift measurement [21]. In the other area [22-31],

many different PS measurements were proposed but less popular then the optical engineering interferometry. For example, associated with attenuation processing, a PS measurement was introduced for industrial applications [22]. Then, by using spectral Foucault technique, a measurement technique of nonlinear temporal phase shifts was proposed [23]. In mechanical engineering, by exploiting a piezoelectric drive, an accurate load detection developed with the PS measurement was initiated [24]. In robotics engineering, an infrared localization in intelligent spaces based on the PS measurement was developed [25]. Then, some innovative applications of PS measurement for laser range finder [26] and pressure variation [27] were also proposed. But, the main focus of the present paper is on the development of RF and microwave range PS measurement technique. In this area, the existing techniques are either expensive as using heterodyne receiver [28], RF modulator [29], narrow band frequency tunable circuitry [30] or differential PS detection modulation [31].

For this reason, we would like to address an innovative and simple technique of PS measurement for ultra-wideband (UWB) applications. In difference to the existing work, the present paper develops an innovative extraction technique of PS (ETPS) dedicated to UWB signals. Practically, the idea consists in combining the unknown PS signal with a reference one through a typically passive topology as T-power divider [32] or active [33] UWB power combiner (PWC). Then, mathematical process is developed to calculate the PS in the wide frequency band. This paper is an English translation of the Chinese reports [34-35].

To overcome this technical challenge, mathematical process is developed in the present paper. In difference to the existing ones, the proposed technique is aimed to calculate the PS in the wide frequency band from the signal magnitudes.

The present paper is organized in four main sections:

- Section 2 describes the fundamental principle of the PS extraction technique.

- Section 3 is the accuracy analysis illustrating the PWC influence onto the extracted PS.
- Section 4 is focused on the validation results with a microstrip circuit proof-of-concept (POC).
- Lastly, Section 5 is the final conclusion.

2. Principle of the PS extraction technique

After the description of the PS extractor circuit configuration, the analytical formulation will be introduced in the present section. Then, realistic case theory by considering S-parameters will be developed.

2.1 PS Extraction in Ideal Configuration

The proposed PS extraction technique is inspired from the geometrical triangulation method. We need three signal vector magnitudes whose two inputs and one output. The output magnitude is measured with a spectrum analyzer (SA). Fig. 1 depicts the illustrative diagram configuration of the proposed PS extraction.

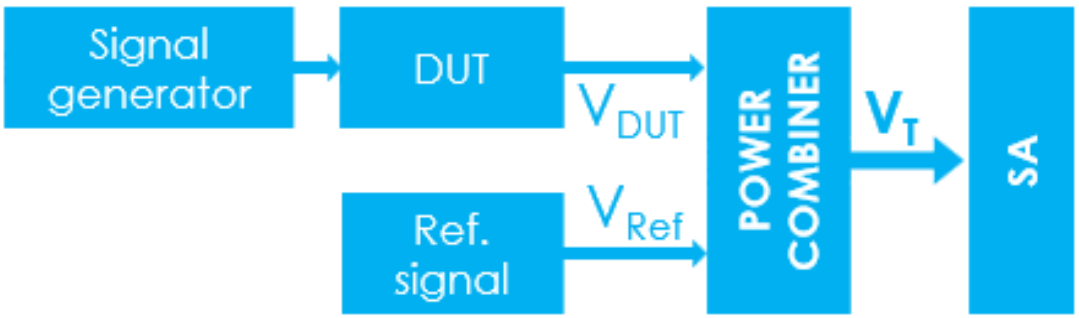

Fig. 1. Principle diagram of the proposed PS extraction.

We suppose that the DUT output as the unknown phase signal. By denoting $j=\sqrt{-1}$ the complex number and ω the angular frequency variable, as operating inputs, let us denote:

- The complex reference signal with magnitude V_{ref} and phase φ_{ref} defined analytically by:

$$\underline{V}_{ref}=V_{ref}\exp[j\varphi_{ref}(\omega)]. \quad (1)$$

- This reference is compared with the complex signal with magnitude V_{DUT} and unknown phase φ_{DUT} expressed in (2). This signal is assumed as an output of a device under test (DUT) attacked by an UWB signal from the generator.

$$\underline{V}_{DUT}=V_{DUT}\exp[j\varphi_{DUT}(\omega)]. \quad (2)$$

Those two signals, assumed completely separated, are injected into the two input ports of three-port PWC. In ideal case, the PWC complex output signal should be equal to:

$$\underline{V}_{T}=\underline{V}_{DUT}+\underline{V}_{ref}. \quad (3)$$

Substituting equation (1) and equation (2) into equation (3), the total signal must be given by:

$$\underline{V}_{T}=V_{DUT}\exp[j\varphi_{DUT}(\omega)]+V_{ref}\exp[j\varphi_{ref}(\omega)]. \quad (4)$$

From this last expression, we can determine $\varphi_{DUT}(\omega)$. The analytical formulation is established from the cosine theorem of arbitrary triangle. Accordingly, the total signal magnitude is written as:

$$V_T^2=\left\{\begin{matrix}V_{DUT}^2+V_{ref}^2+\\2V_{DUT}\cdot V_{ref}\cos\left[\varphi_{DUT}(\omega)-\varphi_{ref}(\omega)\right]\end{matrix}\right\}. \quad (5)$$

2.2 PWC S-Parameters

In practical situation, it is not always easy to realize the circuits able to operate the expression introduced in equation (4). Similar to all RF and microwave engineering concept, it is

necessary to analyze the implemented circuit influence. The reference and DUT signal addition must be realized with the use of three port PWC as illustrated in Fig. 2.

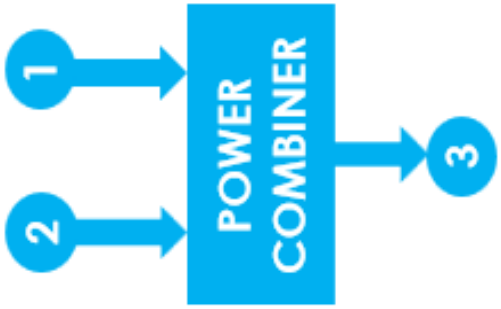

Fig. 2. Three-port PWC black box.

Therefore, the total signal V_T can be unintentionally affected by the PWC imperfection characteristics. To take into account to the PWC influence, we consider the following equivalent S-parameters:

$$[S(j\omega)] = \begin{bmatrix} S_{11}(j\omega) & S_{12}(j\omega) & S_{13}(j\omega) \\ S_{21}(j\omega) & S_{22}(j\omega) & S_{31}(j\omega) \\ S_{31}(j\omega) & S_{32}(j\omega) & S_{33}(j\omega) \end{bmatrix}. \quad (6)$$

In addition to this ideal hypothesis:

$$S_{11,12,13,21,23}(j\omega)=0 \quad (7)$$

the PWC transmission PS accuracy must be negligible. The out of phase difference can be formulated as:

$$\Delta\varphi(\omega) = \left|\varphi_{32}(\omega) - \varphi_{31}(\omega)\right| \approx 0\,. \quad (8)$$

Therefore, the only non-zero elements of the PWC S-matrix must be the transmission coefficients:

$$S_{31}(j\omega) = S_{31}(\omega)\exp\left[\varphi_{31}(\omega)\right] \quad (9)$$

$$S_{32}(j\omega) = S_{32}(\omega)\exp\left[\varphi_{32}(\omega)\right]. \quad (10)$$

2.3 Analytical Formulation of the Proposed PS Extraction

Consequently, by introducing the PWC parameter effect, the total voltage V_T expressed in (4) should be approximated as:

$$\underline{V}_T \approx \underline{\alpha}_{ref} \cdot \underline{V}_{ref} + \underline{\alpha}_{DUT} \cdot \underline{V}_{DUT} \tag{11}$$

It means that, the total signal $\underline{V}_T$ magnitude is written as:

$$V_T^2 = \left\{ \begin{matrix} \alpha_{DUT}^2 V_{DUT}^2 + \alpha_{ref}^2 V_{ref}^2 + \\ 2\alpha_{DUT}\alpha_{ref} V_{DUT} V_{ref} \cos\left[\varphi_T(\omega)\right] \end{matrix} \right\} \tag{12}$$

where:

$$\varphi_T(\omega) = \varphi_{ref}(\omega) - \varphi_{21}(\omega) - \varphi_{31}(\omega)\,. \tag{13}$$

It yields that the unknown PS can be formulated by:

$$\varphi_{DUT}(\omega) = \arccos\left[\frac{V_T^2 - \alpha_{DUT}^2 V_{DUT}^2 - \alpha_{ref}^2 V_{ref}^2}{2\alpha_{DUT}\alpha_{DUT} V_{DUT} \cdot V_{ref}} \right] + \varphi_T(\omega)\,. \tag{14}$$

3. ILLUSTRATIVE CASE STUDY

Two illustrative cases of ideal applications depending on the PWC S-parameters is described in the present section. The first case is the consideration of the completely matched and isolated PWC. The other case is the application with unmatched and non-isolated PWC. The sensitivity analyses of the reflection and isolation coefficients onto the unknown PS $\varphi_{DUT}(\omega)$ will be studied.

3.1 Illustrative Case 1: PS Extraction with Ideal DUT

In this case, a basic simulation method is used to validate our PS extraction technique. The simple idea is shown in Fig. 1 is implemented into the concrete circuit schematic depicted in Fig. 3. It can be reminded that we need one signal source works as reference signal (V_{REF}) to input of power combiner, the other signal source excites the DUT, and the output of DUT (V_{DUT}) is connected to the input of PWC. Then, the output signal of the latter denoted V_T will be exploited to obtain the unknown PS. With circuit simulation software ADS® from Keysight Technologies®, a TL assigned with physical length d=7.5 cm with characteristic and reference impedance R_0=50 Ω is used as the DUT. The ideal PWC is represented by the S-parameter black box:

$$[S(j\omega)] = \begin{bmatrix} 0 & 0 & 0.5 \\ 0.5 & 0 & 0.5 \\ 0 & 0 & 0 \end{bmatrix}. \tag{15}$$

Thus, the touchstone S-parameters model of commercial devices with reference Mini-circuits ZFRSC-123-S+ was also used as a real PWC. It is assumed perfect which the reflection and isolation are equal to zero. The simulation principle is shown in Fig. 3, with the magnitude of V_T, V_{DUT}, V_{ref} and the phase of φ_{ref}, the phase of TL φ_{DUT} is calculated using equation (14).

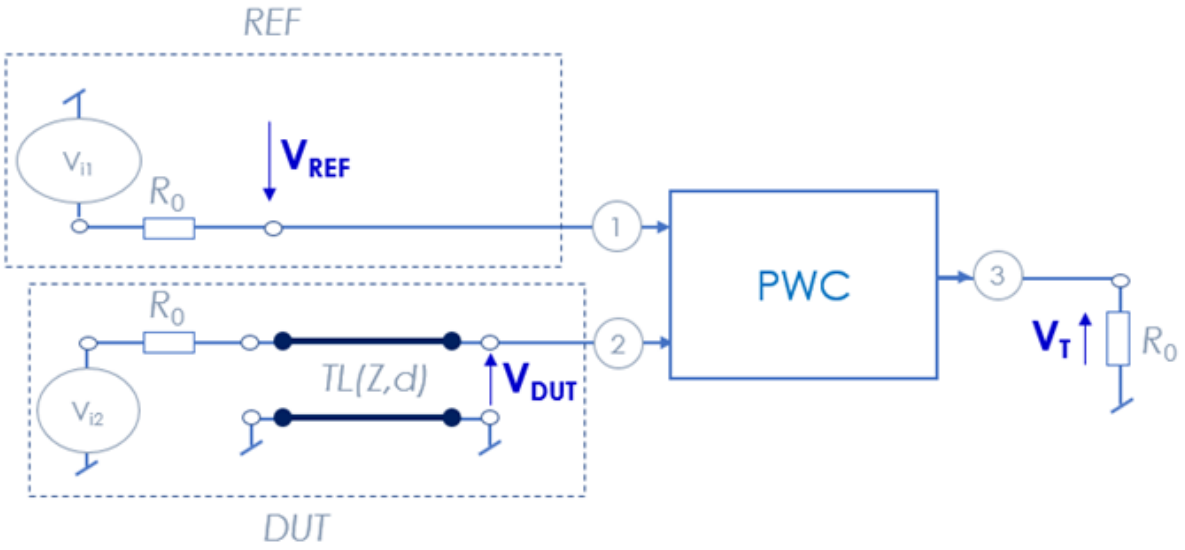

Fig. 3. Schematic of the PS extractor circuit design in the SPICE ADS® environment.

Then, the ADS simulation ("Simu.") result and theory result in the super UWB from DC to 4 GHz are compared, as shown in Figs. 4. A good agreement between the PS from ideal (Fig. 4(a)) and ideal (Fig. 4(b)) PWC was obtained. As expected, the behavioral PS of TL with perfect linear decrease from 0° with slope corresponding to the group delay 1.6 ns of about is observed. It can be underlined that they are very well matched with absolute inaccuracy error lower than $|\varphi_{Simu}(f)-\varphi_{calculated}(f)|<0.1°$ in the whole considered frequency band. This result allows to understand and pre-validated the PS extraction feasibility in simulation environment.

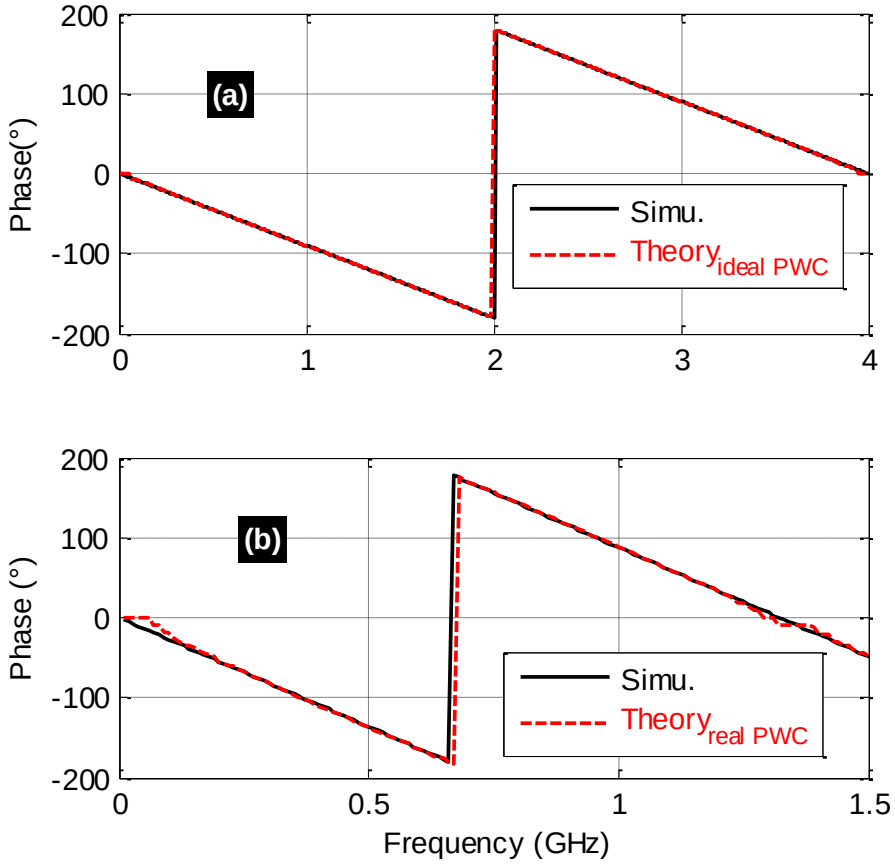

Fig. 4. Comparison between the calculated and simulated PS: (a) ideal and (b) real PWC.

4.2 Illustrative Case 2: Influence of PWC Reflection and Isolation Coefficients

In the previous subsection, the ideal model of perfectly matched and isolated access PWC is used, but it doesn't exist in real world. One may curiously wonder about the influence of the reflection and isolation on the phase extraction method. Therefore, it is keen to study this aspect in the present subsection.

4.2.1 Influence of PWC Reflection Coefficient on PS Accuracy

By hypothesis, we are dealing with the case of the ideal power combiner presenting the reflection coefficient denoted R_{edB} in this paragraph. The S-matrix equivalent model of PWC is expressed as:

$$[S(j\omega)] = \begin{bmatrix} R_e & 0 & 0.5 \\ 0.5 & R_e & 0.5 \\ 0 & 0 & R_e \end{bmatrix}. \quad (16)$$

It is varied from 20 dB to 60 dB during the simulation. The cartography mapping of Fig. 5(a) highlights clearly how the PS varies with the PWC reflection. As shown in Fig. 5(b), the calculated and simulated PS discrepancies $|\varphi_{Simu}(f) - \varphi_{calculated}(f)|$ increases with R_e.

As pointed out in Table I, with 20 dB reflection, the calculated PS presents about $|\varphi_{Simu}(f) - \varphi_{calculated}(f)| = 10°$ differences when compared to the simulation phase result. If the PWC reflection has 40 dB, the error between the theory and simulation is about 1° or 2°. 60 dB reflection parameter makes the theory perfectly matched with the simulation results.

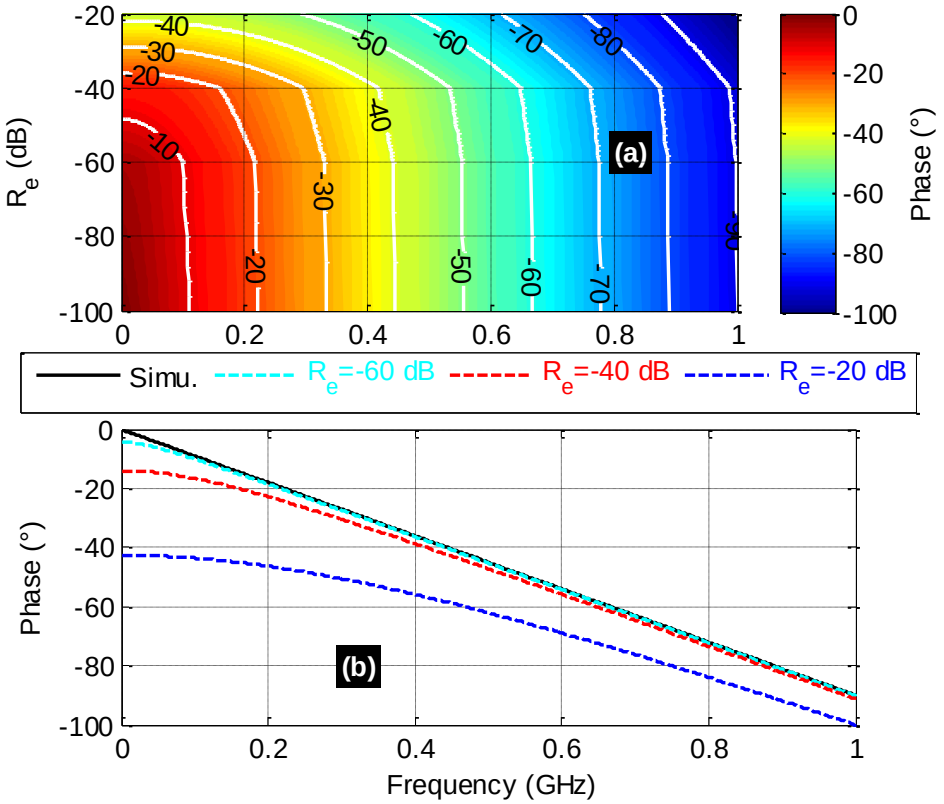

Fig. 5. PWC reflection influence on the PS accuracy.

TABLE I. INFLUENCE OF THE PWC REFLECTION COEFFICIENT ON THE CALCULATED DUT PS ACCURACY.

R_e (dB)	-60	-40	-30	-20
$\Delta\varphi_{min}$	0.01	0.1	4	7
$\Delta\varphi_{max}$	1.5	10	14	42

4.2.2 Influence of PWC Isolation Coefficient on PS Accuracy

The present paragraph investigates the PS accuracy with respect to the isolation I_s. Doing this, the PWC is modelled by the S-parameter black box:

$$[S(j\omega)] = \begin{bmatrix} 0 & I_s & 0.5 \\ I_s & 0 & 0.5 \\ I_s & I_s & 0 \end{bmatrix}. \qquad (17)$$

The ideal power combiner with the isolation between the two inputs varies from 20 dB to 60 dB is used in the simulation. The cartography mapping of Fig. 6(a) highlights clearly how the PS varies with the PWC isolation imperfection. As shown in Fig. 6(b), the calculated PS error increases with I_s. As mentioned in Table II, if the power combiner has 20 dB isolation, the error between theory and simulation is $|\varphi_{Simu}(f)-\varphi_{calculated}(f)|_{\max}$ =10° in low frequencies, and $|\varphi_{Simu}(f)-\varphi_{calculated}(f)|_{\max}$ =5° in high frequencies.

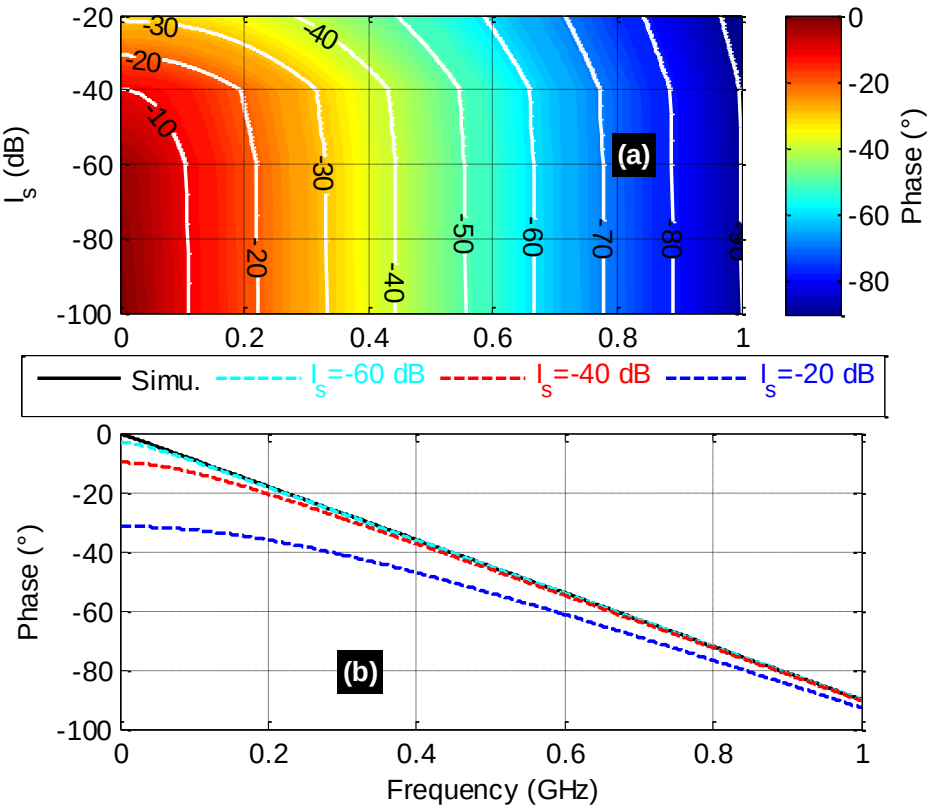

Fig. 6. PWC isolation influence on the PS accuracy.

TABLE II. INFLUENCE OF THE PWC ISOLATION COEFFICIENT ON THE CALCULATED DUT PS ACCURACY.

I_s (dB)	-60	-40	-30	-20
$\Delta\varphi_{min}$	0.01	0.1	1	3

$\Delta\varphi_{max}$	1	9	13	31

If the power combiner reflection has 40 dB, the error between the theory and simulation is well matched in high frequency. Compared to isolation, power combiner reflection is more important to the phase extraction method.

To validate experimentally the established PS extraction technique, measurement investigation will be discussed in the following section.

5. EXPERIMENTAL VALIDATION

In this section, the PS extraction frequency domain experimentation will be described. Then, the obtained results will be discussed.

5.1 Experimental Setup Description

Fig. 7(a) represents the illustration diagram of experimental setup. A signal generator was used to provide the reference and the DUT input signals. The corresponding photograph is depicted in Fig. 7(b). The measurements were carried out with the experimental setup using signal generator N9310A and SA MXE N9038A from Keysight Technologies®. We choose the DUT as a 50-cm long coaxial cable.

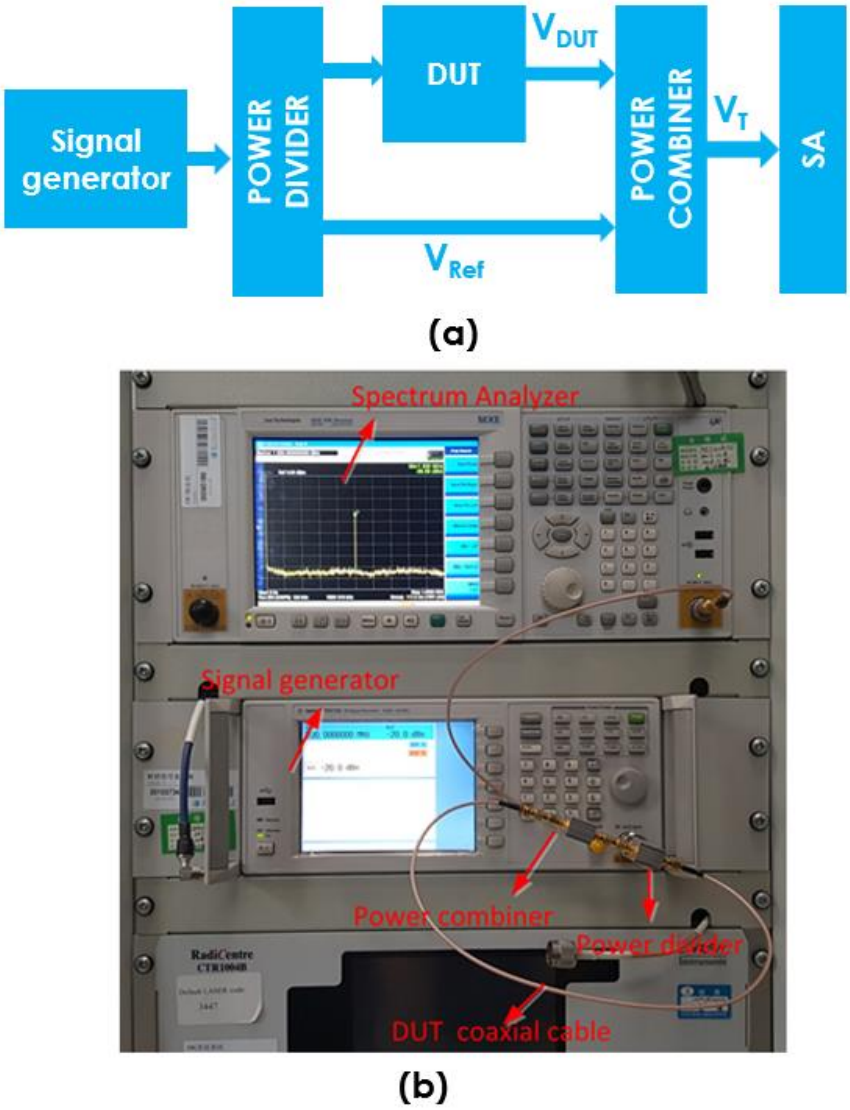

Fig. 7. Experimental setup of the PS extraction technique POC.

5.2 Discussion on Measured Results

The employed PWD and PWC are commercial devices with reference Mini-circuits ZFRSC-123-S+. These three port devices have transmission coefficients S_{31} and S_{32} as plotted in Fig. 8. The reflection and isolation coefficients are better than -30 dB and -19 dB, respectively.

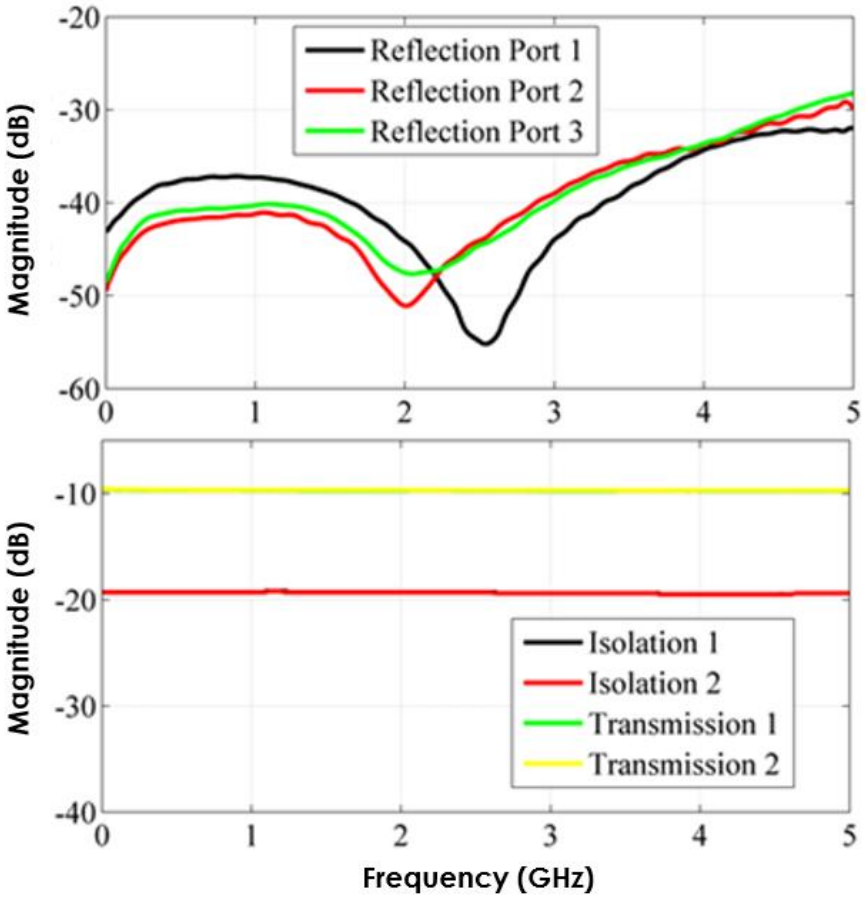

Fig. 8. (a) PS extraction POC experimental setup and (b) PWC S parameters.

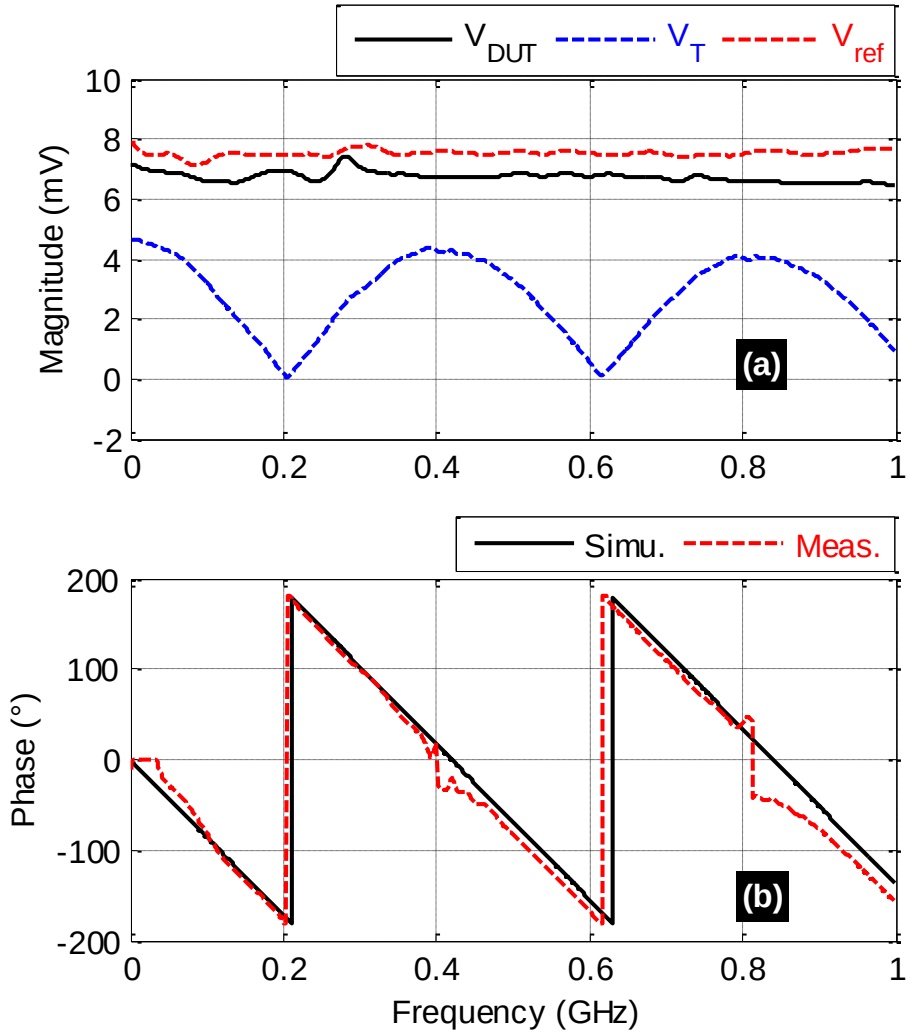

Fig. 9. (a) DUT, ref. and combined measured signal magnitudes and (b) comparisons of calculated and simulated PS.

The measurement tests were carried out in three steps successively with ref., DUT and total signals. The measured signal magnitudes from 3 Hz to 0.6 GHz are displayed in Fig. 9(a). The combined signal has a periodical aspect. The obtained PSs are sketched in Fig. 9(b). The calculated PS from equation (14) using the measured ("Meas.") signal magnitudes matches very well with ADS® simulations ("Simu."). The maximal absolute deviation is less than 5° in the considered frequency band.

4. Conclusion

A PS extraction technique based on arbitrary and UWB signal magnitude spectrum measurement is developed. The analytical principle is described. The analytical formulation of the PS in function of the operating signal magnitudes is established from the geometrical cosine theorem.

To verify the feasibility of the technique, accuracy analyses with respect to the used PWC parameters are performed. Then, experimental validation is performed with consideration of commercial PWC device. As expected, the calculated PS results from measurement and simulations in super UWB frequency from 3 Hz to 0.6 GHz are in good correlation.

References

[1] N. W. Harris, “Dynamic Phase Shift Measurement,” Proceedings of the IEEE, Vol. 54, No. 12, 1966, pp. 1979 – 1979.

[2] T. Kawakami, “Microwave Attenuation and Phase-Shift Measurement Using Stepped Phase Modulation,” IEEE Trans. Instrumentation and Measurement, Vol. 27, No. 1, 1978, pp. 33 – 38.

[3] Hong-Teuk Kim, Sanghyo Lee, Sungwon Kim, Youngwoo Kwon and Kwang-Seok Seo, “Millimetre-wave CPS distributed analogue MMIC phase shifter,” Electronics Letters, Vol. 39, No. 23, Nov. 2003, p. 1661.

[4] David M. Zaiden, John E. Grandfield, Thomas M. Weller and Gokhan Mumcu, “Compact and Wideband MMIC Phase Shifters Using Tunable Active Inductor-Loaded All-Pass Networks,” IEEE Trans. Microwave Theory and Techniques, Vol. 66, No. 2, Feb. 2018, pp. 1047-1057.

[5] M. S. Rabbani and H. Ghafouri-Shiraz, “Evaluation of gain enhancement in improved size microstrip antenna arrays for millimetre-wave applications,” AEU - Int. J. Electron. Commun., Vol. 81, 2017, pp. 105-113.

[6] You Zheng and Carlos E. Saavedra, “Full 360∘ Vector-Sum Phase-Shifter for Microwave System Applications,” IEEE Trans. on Circuits and Systems I: Regular Papers, Vol. 57, No. 4, Apr. 2010, pp. 752–758.

[7] B. Ravelo, “Distributed NGD active circuit for RF-microwave communication,” AEU - Int. J. Electron. Commun., Vol. 68, No. 4, Apr. 2014, pp. 282-290.

[8] Q. Zhao and G. L. Stuber, "Robust time and phase synchronization for continuous phase modulation," IEEE Transactions on Communications, Vol. 54, No. 10, Oct. 2006, pp. 1857-1869.

[9] Y. Liu and B. Ravelo, "Fully time-domain scanning of EM near-field radiated by RF circuits," Progress In Electromagnetics Research (PIER) B, Vol. 57, 2014, pp. 21-46.

[10] I. Rodríguez-Rodríguez, J. V. Rodríguez and L. Juan-Llácer, "Validation with measurements of plane and spherical-wave UTD-PO propagation models which assume flat-topped obstacles," AEU - Int. J. Electron. Commun., 85, 2018, pp. 174-178.

[11] Fei Liu, Qinghai Yang, Qingsu Heb Kyung and Sup Kwak, "Energy efficiency and spectral efficiency tradeoff in downlink OFDMA systems with imperfect CSI," AEU - Int. J. Electron. Commun., Vol. 85, 2018, pp. 54-58.

[12] Gwan-Bon Koo; Gun-Woo Moon; Myung-Joong Youn, "New zero-voltage-switching phase-shift full-bridge converter with low conduction losses," IEEE Transactions on Industrial Electronics, Vol. 52, No. 1, Feb. 2005, pp. 228–35.

[13] H. Zhang, T. Banno, Y. Mitsuya and K. Fukuzawa, "Direct Visualization of Molecularly Thin Lubricant Films Using Low-Coherence Phase-Shifting Interferometry," in Proc. of Asia-Pacific Magnetic Recording Conference 2006, Singapore, Singapore, 29 Nov.-1 Dec. 2006, pp. 1-2.

[14] X. F. Xu, L. Z. Cai, Y. R. Wang, X. F. Meng, W. J. Sun, H. Zhang, X. C. Cheng, G. Y. Dong, and X. X. Shen, "Simple direct extraction of unknown phase shift and wavefront reconstruction in generalized phase-shifting interferometry: algorithm and experiments," Optics Letters, Vol. 33, No. 8, Apr. 15, 2008, pp. 776-778.

[15] G. Rodriguez-Zurita, N.I. Toto-Arellano, C. Meneses-Fabian and J. F. Vazquez-Castillo, "Lateral and rotational shearing phase-shifting interferometry with phase-grating

multiplexing," in Proc. of 2009 Conference on Lasers & Electro Optics & The Pacific Rim Conference on Lasers and Electro-Optics, Shanghai, China, 30-3 Aug. 2009, pp. 1-2.

[16] G. Rodriguez-Zurita, N. I. Toto-Arellano, M. L. Arroyo-Carrasco, C. Meneses-Fabian and J. F. Vazquez Castillo, "Experimental observation of spiral patterns by obstruction of Bessel beams: Application of single shot phase-shifting interferometry," in Proc. of 2009 Conference on Lasers & Electro Optics & The Pacific Rim Conference on Lasers and Electro-Optics, Shanghai, China, 30-3 Aug. 2009, pp. 1-2.

[17] Roma Jang, Jae Wan Kim, Chu-Shik Kang, Jong-Ahn Kim, Tae Bong Eom, Jae-Eun Kim and Hae Yong Park, "Frequency scanning laser for high speed phase shifting interferometry," In Proc. of 2009 Conference on Lasers and Electro-Optics and 2009 Conference on Quantum electronics and Laser Science Conference, Baltimore, MD, USA, 2-4 June 2009, pp. 1-2.

[18] Zhuo Li and Xiaoxu Lu, "Efficient Iterative Algorithm with Unknown Reference Phases in Phase Shifting Interferometry," In Proc. of 2011 Symposium on Photonics and Optoelectronics (SOPO), Wuhan, China, 16-18 May 2011, pp. 1-4.

[19] V. I. Guzhov, S. P. Ilinykh, D. S. Haydukov and R. A. Kuznetzov, "Decoding algorithm for interference patterns in phase shifting interferometry without a priori shift knowledge," In Proc. of 2012 7th International Forum on Strategic Technology (IFOST), Tomsk, Russia, 18-21 Sept. 2012, pp. 1-4.

[20] D. Ghareab and A. Ibrahim, "Quadrature phase-shifting interferometry for surface micro-topography measurement," In Proc. of 2017 Conference on Lasers and Electro-Optics Pacific Rim (CLEO-PR), 31 July-4 Aug. 2017, Singapore, Singapore, pp. 1-2.

[21] Y. Yamanaka, G. Sakano, J. Haruki and K. Kato, "THz-wave phase shift measurement by THz-wave interferometer," Electronics Letters, Vol. 53, No. 13, June 2017, pp. 868–869.

[22] J. Kalinski, "A Chopped Subcarrier Method of Simultaneous Attenuation and Phase-Shift Measurement under Industrial Conditions," IEEE Transactions on Industrial Electronics and Control Instrumentation, Vol. IECI-28, No. 3, 1981, pp. 201 – 209.

[23] C. Dorrer, "Measurement of nonlinear temporal phase shifts using spectral Foucault technique," Electronics Letters, Vol. 42, No. 11, 2006, pp. 649 – 650.

[24] Carsten Wallenhauer, Bernhard Gottlieb, Andreas Kappel, Tim Schwebel, Johannes Rucha and Tim Luth, "Accurate Load Detection Based on a New Piezoelectric Drive Principle Employing Phase-Shift Measurement," Journal of Microelectromechanical Systems, Vol. 16, No. 2, 2007, pp. 344-350.

[25] E. Martín-Gorostiza, F. J. Meca Meca, J. L. Lázaro Galilea, D. Salido Monzú, Luis Pallarés Puerto and Ana Moral Alcaraz, "Error corrections in phase-shift measurement for robot infrared localization in intelligent spaces," In Proc. of 2009 IEEE International Workshop on Robotic and Sensors Environments, Lecco, Italy, 6-7 Nov. 2009, pp. 1-6.

[26] L. Gatet and H. Tap-Beteille, "Measurement Range Increase of a Phase-Shift Laser Rangefinder Using a CMOS Analog Neural Network," IEEE Trans. on Instrumentation and Measurement, Vol. 58, No. 6, 2009, pp. 1911 – 1918.

[27] Zhiyong Luo and Chi Chen, "Phase-shifting interferometry: A method for generating phase shifting by pressure variation," In Proc. of CPEM 2010, Daejeon, South Korea, 13-18 June 2010, pp. 502-503.

[28] T. Y. Wu, "Accurate measurement of microwave phase-shift from 2 to 18 GHz using heterodyne receiver," Electronics Letters, Vol. 47, No. 14, 2011, pp. 802 – 804.

[29] Javier Urricelqui, Ander zornoza indart, Mikel Sagues and Alayn Loayssa, "Dynamic BOTDA measurements based on Brillouin phase-shift and RF demodulation," Optics Express, Vol. 20, No. 24, Nov. 2012, pp. 26942-26949.

[30] Xuejian Wu, Yan Li, Haoyun Wei and Jitao Zhang, "Phase-shifting interferometry to determine the absolute diameter of a silicon sphere using a frequency-tunable diode laser," In Proc. of 2013 Conference on Lasers & Electro-Optics Europe & International Quantum Electronics Conference CLEO EUROPE/IQEC, Munich, Germany, 12-16 May 2013, pp. 1.

[31] X. Gu, S. V. Marchese and K. Bohnert, "Robust non-reciprocal optical DC phase shift measurement with differential modulation phase detection," in Proc. of 2015 Conference on Lasers and Electro-Optics (CLEO), San Jose, CA, USA, 10-15 May 2015, pp. 1-2.

[32] B. Ravelo, "Modelling of asymmetrical interconnect T-tree laminated on flexible substrate," Eur. Phys. J. Appl. Phys. (EPJAP), Vol. 72, No. 2 (20103), Nov. 2015, pp. 1-9.

[33] B. Ravelo, "Synthesis of N-way active topology for wide-band RF/microwave applications," International Journal of Electronics (IJE), Vol. 99, No. 5, May 2012, pp. 597-608.

[34] Fayu Wan and Fangfang Liu, "Phase measurement method for arbitrary wideband signals based on amplitude measurement," Electrical Measurement & Instrumentation, online, in Chinese, 2019.

[35] F. Liu, "Phase measurement method for arbitrary wideband signals based on amplitude measurement," Master Thesis, NUIST, Nanjing, China, 2019.